

Chapter 13

Investigating Fourteen Years of Net Primary Productivity Based on Remote Sensing Data for China

Christina Eisfelder and Claudia Kuenzer

Abstract Net primary productivity (NPP) is an important environmental indicator that provides information about vegetation productivity and carbon fluxes. Analyses of NPP time-series allow for understanding temporal patterns and changes in vegetation productivity. These are especially important in rapidly changing environments, such as China, the world's third largest country. In this study, we use the model BETHY/DLR (Biosphere Energy Transfer Hydrology Model) for derivation of NPP time-series for China for 14 years from 1999–2012. We analyse spatial and temporal NPP distributions. These include mean annual NPP distribution and mean productivities for different land cover classes. Monthly data provide information about temporal patterns of vegetation productivity for different regions in China and different vegetation types. Analyses of interannual NPP variability revealed considerable differences in the development of annual vegetation productivity within the analysed time period for different provinces. The decrease in NPP for the district Shanghai shows the strong influence of one of Asia's fastest growing megacities on the environment. The NPP time-series was additionally analysed for a forest region in North China, which has been affected by forest disturbances. Our results show that the NPP data are suitable for monitoring of forest disturbance and regrowth. The analyses and results presented in this study provide valuable information about spatial and temporal variation of vegetation productivity in the various regions within China.

C. Eisfelder (✉) • C. Kuenzer
German Remote Sensing Data Center, DFD, Earth Observation Center, EOC,
German Aerospace Center, DLR, Oberpfaffenhofen, Germany
e-mail: Christina.Eisfelder@dlr.de

13.1 Introduction

Net primary productivity (NPP) is the dry matter production by vegetation. It quantifies the carbon uptake by plants per unit area and unit time and, thus, provides information about carbon emission or sequestration. NPP is a key variable for ecological and environmental monitoring and a sensitive indicator of climate change (Niemeijer 2002; Schimel 1995). It plays an important role in the global carbon cycle (Prentice et al. 2001).

Modelling of NPP is of special interest in a country that shows such immense and rapid development like China (United Nations Development Programme UNDP 2013). The People's Republic of China is the world's third largest country and also the most populous (Population Reference Bureau, PRB 2013). It experiences strong economic growth and migration trends, which put pressure on ecological resources (PRC 2012).

Monitoring of NPP and its spatio-temporal dynamics are important base information for understanding possible impacts of global change and land management (Eisfelder et al. 2014). In the past decade, several studies on NPP estimation for China have been published, but most focus on small study areas or short time-periods (e.g. Fu et al. 2013; Gao et al. 2013; Lu et al. 2013). National wide studies are fewer and do so far not present variations for the first decade of twenty-first century (Cao et al. 2003; Gao et al. 2004; Hou et al. 2013).

In this study, we model NPP for China for the 14-year period from 1999 to 2012. We apply the remote sensing data based Biosphere Energy Transfer Hydrology (BETHY/DLR) model. Our aims were to present annual NPP distribution for the period 1999–2012 for China, analyse monthly patterns of vegetation productivity, and investigate interannual variations in NPP for the time period covered. We also analyse whether the modelled NPP data can be used for monitoring of forest disturbance areas in North China. Thereby, we want to demonstrate the usability of the modelled NPP time-series for understanding patterns in NPP and for monitoring possible long-term changes in vegetation productivity.

13.2 Data and Methods

In this chapter, we introduce the study area and provide a short description of the NPP model used within this study.

13.2.1 Study Area

Our study area is the People's Republic of China. China covers an area of about 9.6 million km². It is one of the world's largest countries and encompasses diverse

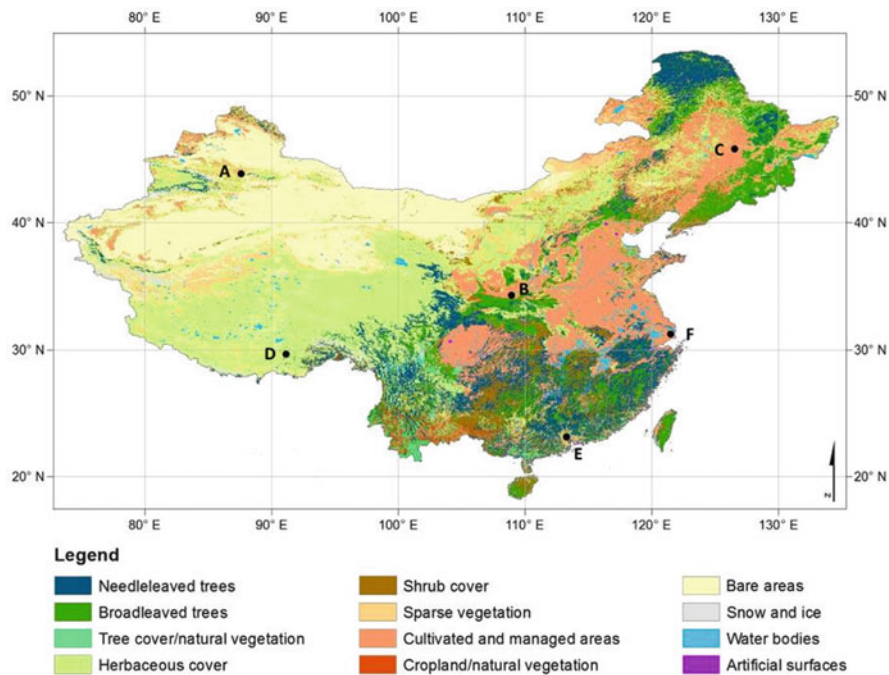


Fig. 13.1 Land cover for China from the GLC2000 (Bartholomé and Belward 2005; with simplified legend). Locations A–F refer to the precipitation and temperature diagrams from Fig. 12.2

climatic conditions. Figure 13.1 gives an overview on the land cover of China according to the land cover classification from the global land cover database for the year 2000 (GLC2000) (Bartholomé and Belward 2005).

In the western part of the country, grassland and sparsely vegetated areas are dominant. In the northeast boreal forest and agricultural areas can be found. The largest agricultural areas are located in the central eastern part of China. The regions in the southeast are mainly covered by a mixture of natural vegetation, mainly forest areas, shrub cover, and some agricultural areas (compare Fig. 13.1).

The southeastern part of China can be described as a warm temperate climate with fully humid to winter dry conditions and hot to warm summers (Kottek et al. 2006). In the northeastern part of the country snow climate with dry winters and hot to warm summers is dominant. The western part of China can be divided into a cold arid desert climate in the northern part and a polar tundra climate in the southern part including the Tibetan plateau (Kottek et al. 2006). Figure 13.2 shows selected precipitation and temperature diagrams for different regions of the country (locations given in Fig. 13.1).

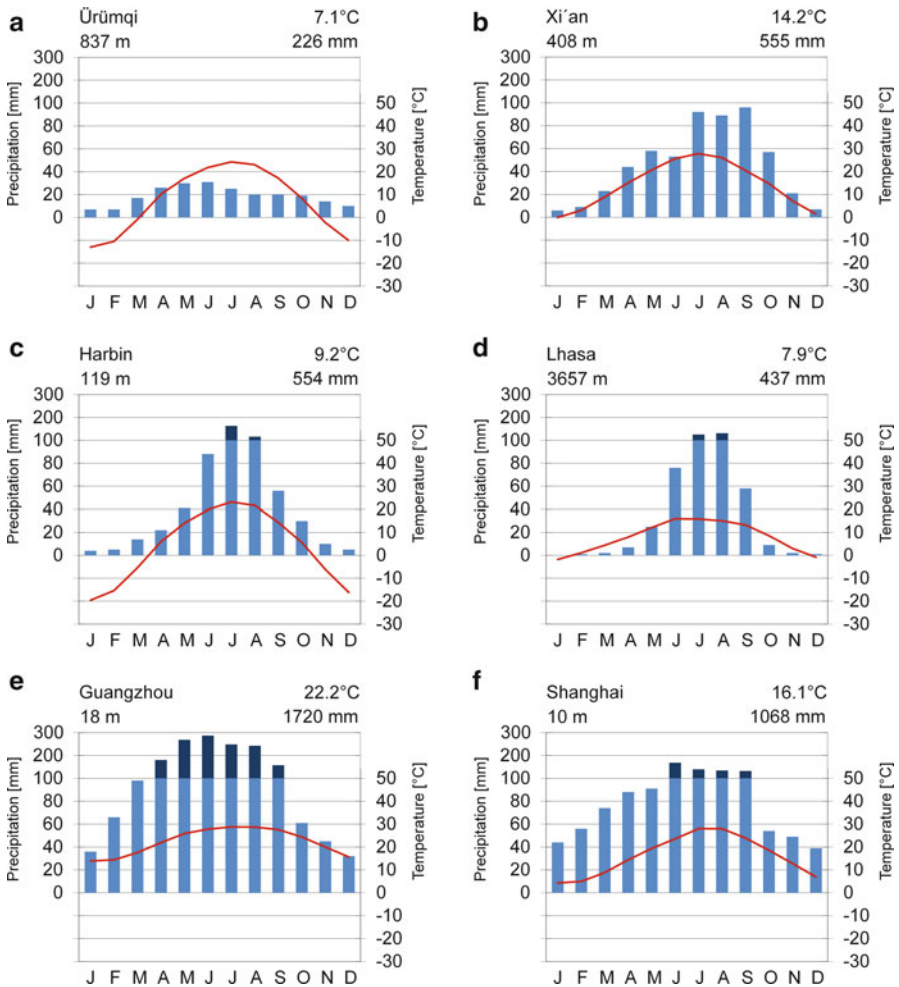


Fig. 13.2 Selected precipitation (average monthly precipitation) and temperature (average daily mean temperature) diagrams (extracted from Hijmans et al. 2005). Locations of the diagrams (a–f) are shown in Fig. 13.1: (a) Ürümqi, (b) Xi'an, (c) Harbin, (d) Lhasa, (e) Guangzhou, (f) Shanghai

13.2.2 The Model BETHY/DLR

In this study, we applied the model BETHY/DLR for NPP calculation for China. BETHY/DLR is a soil-vegetation-atmosphere-transfer (SVAT) model (Wißkirchen et al. 2013). It is based on meteorological and remote sensing derived input data. The CO_2 uptake by vegetation is simulated by BETHY/DLR as a process that is limited by light intensity, heat, and soil water availability (Knorr 1997). The parameterization of photosynthesis distinguishes between C_3 and C_4 plants (Farquhar et al. 1980; Collatz et al. 1992). The photosynthesis rate A is defined as the

minimum of the carboxylation rate and the electron transport rate, minus dark respiration (Eisfelder et al. 2014).

BETHY/DLR currently differentiates 33 internal vegetation types, for which individual plant specific parameters are provided. These are needed for calculation of photosynthesis and include maximum carboxylation rate, maximum electron transport rate, maximum rooting depth, and maximum height. For each spatial unit (i.e. pixel), two vegetation types can be modelled. This allows modelling of mixed land cover classes as well as representation of fractional coverage of less than 100 %. Weighting factors define the fraction of primary and secondary vegetation type (Eisfelder et al. 2013; Wißkirchen et al. 2013).

BETHY/DLR is driven by meteorological and remote sensing based input data (Table 13.1). Meteorological data are available from the European Centre for Medium-Range Weather Forecasts (ECMWF) ERA-Interim reanalysis (Berrisford et al. 2011; Dee et al. 2011). These include data on precipitation, air temperature, cloud coverage, and wind speed. Further, a land cover map and leaf area index (LAI) data are used. The GLC 2000 (Bartholomé and Belward 2005) land cover map was used within this study. Remote sensing based LAI data were available from the geoland2 (Gio-GL 2013) data base. The LAI data are available globally and provided with 1 km² resolution as 10-day composites. Pre-processing of LAI time-series was performed before the data were used as input for BETHY/DLR. This included correction of gaps and outliers in the time-series with a harmonic analysis (Wißkirchen et al. 2013).

Additional input data for BETHY/DLR comprise a digital elevation model from the latest version of the NOAA/NGDC GTOPO30 product (USGS 1996) and soil types from the FAO soil map (FAO et al. 2009).

The spatial resolution of the NPP output from BETHY/DLR is 1 km². This equals the resolution of LAI and land cover input data. The continuous time-series of meteorological input data on at least daily basis (cf. Table 13.1) allows for a high temporal resolution. NPP outputs are calculated daily. Based on these daily data, monthly and annual sums and means are calculated. An overview on the processing scheme of BETHY/DLR is provided in Fig. 13.3.

13.3 Results and Discussion of NPP for China

Based on the monthly and annual NPP data, we analysed the spatial distribution of vegetation productivity in China and calculated productivities for individual land cover classes. Further, we discuss the monthly development of NPP and have a look at interannual variations in vegetation productivity.

Table 13.1 Input data for NPP modelling with BETHY/DLR for China

Input parameter	Spatial resolution	Temporal resolution	Source
Land cover map	~1 km	Once	GLC2000
LAI	~1 km	10-daily	geoland2
Soil map	~1 km	Once	FAO
Digital elevation model	~1 km	Once	GTOPO30
2 metre temperature	0.25°	>daily	ECMWF
Large-scale and convective precipitation	0.25°	>daily	ECMWF
Low, medium, and high cloud cover	0.25°	>daily	ECMWF
10 metre eastward and northward wind component	0.25°	>daily	ECMWF
Surface geopotential	0.25°	Once	ECMWF

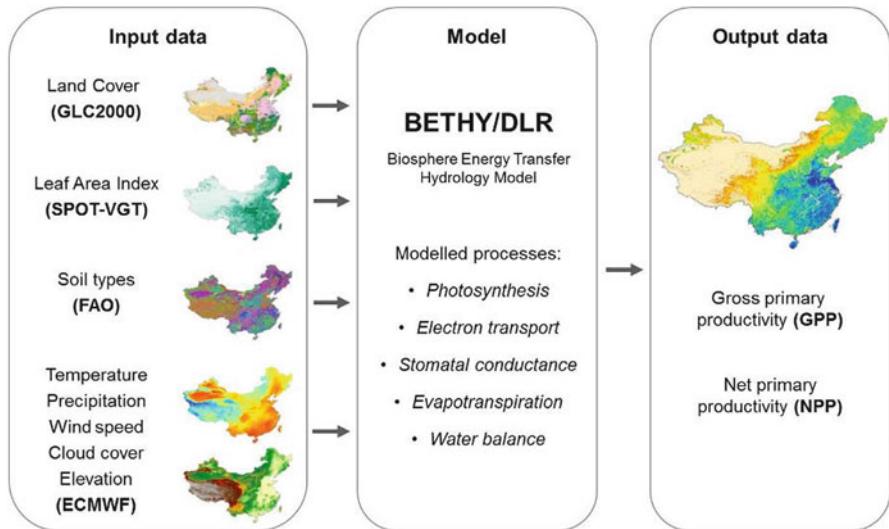


Fig. 13.3 Scheme of BETHY/DLR model

13.3.1 Spatial NPP Distribution

Figure 13.4 presents the calculated mean annual NPP for China for 1999–2012. Highest mean annual NPP values can be observed in areas covered by broadleaved forest or shrubs in the south-eastern part of China. In these areas, annual NPP sums range between 1,500 and 2,000 g C m⁻². Agricultural areas in the central eastern part of the country, roughly located between 32–36°N and 113–121°E, also show high NPP with productivity maxima reaching 1,500 g C m⁻².

The western part of China, a region covered by herbaceous vegetation, sparse vegetation, and bare areas (cf. Fig. 13.1), is characterized by very low vegetation

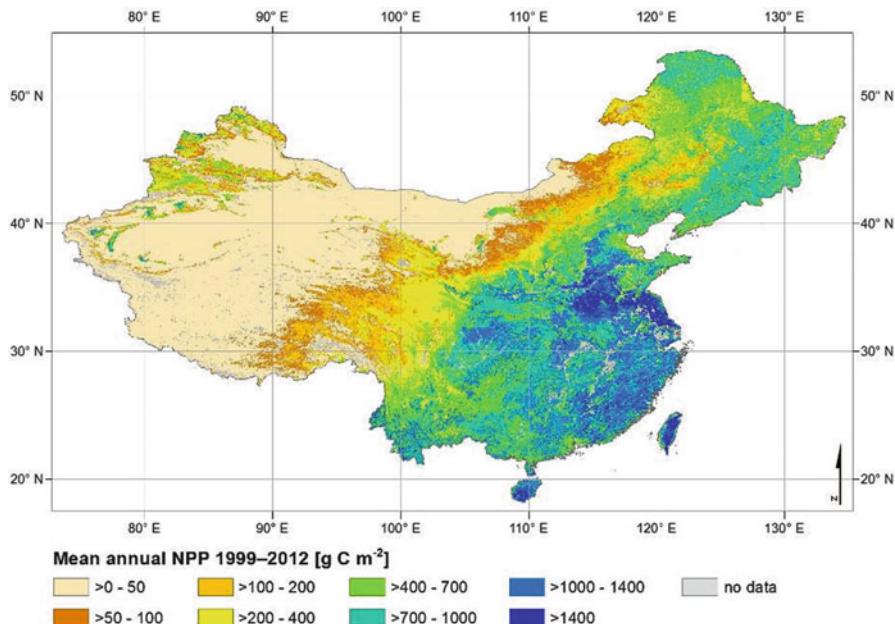


Fig. 13.4 Mean annual NPP for China for 1999–2012 calculated with BETHY/DLR

productivity. In the area between 37–42°N and 75–87°E some local spots with clearly visible higher productivity can be observed. These are cultivated and managed areas (cf. Fig. 13.1) and, further north, also some more grassland and managed areas can be identified. In addition, Fig. 13.5 provides an overview on average mean annual NPP values for individual provinces within China.

Average mean annual NPP values for individual land cover classes are presented in Table 13.2. Highest productivity can be observed for broadleaved evergreen and trees with NPP of 1,034 g C m⁻². This is followed by cultivated and managed areas (824 g C m⁻²), broadleaved deciduous trees (718 g C m⁻²), needleleaved trees (707 g C m⁻², 704 g C m⁻²) and evergreen shrubs (686 g C m⁻²). Lowest annual NPP in the period 1999–2012 have herbaceous cover (171 g C m⁻²), sparse vegetation (57 g C m⁻²), and bare areas (18 g C m⁻²).

The NPP values from BETHY/DLR presented in Table 13.2 correspond to productivities published in other studies for China. Feng et al. (2007), for example, reported annual NPP values of 122.6 g C m⁻² for grassland, 14.3 g C m⁻² for barren areas, 342 g C m⁻² for cropland, 363 g C m⁻² for shrubland, and 552 g C m⁻² at average for forests. Yan et al. (2006) found annual NPP for coniferous and broadleaf mixed forest in the Dinghushan Biosphere Reserve of 1,148 g C m⁻² for evergreen broad-leaf forest and 678 g C m⁻².

Matsushita and Tamura (2002) reported NPP of 1178 g C m⁻² for broadleaved forests, 690 g C m⁻² for broadleaved crops, 614 g C m⁻² for needleleaved forest, and 460 g C m⁻² for shrubs in East Asia. For grasslands in western China

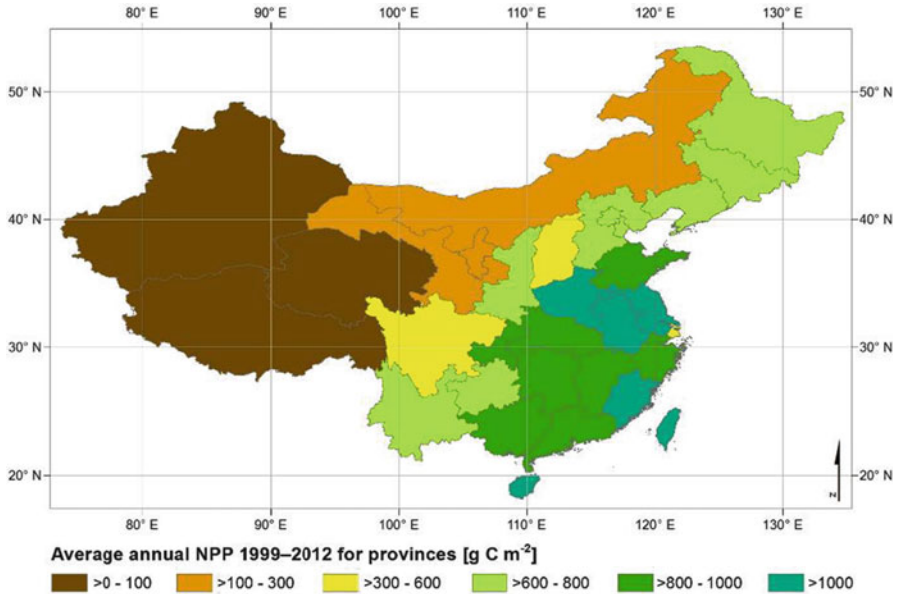


Fig. 13.5 Mean annual NPP for individual provinces within China for 1999–2012 calculated with BETHY/DLR

Table 13.2 Average mean annual NPP for different land cover types in China for 1999–2012

Land cover type	Mean annual NPP [g C m ⁻²]
Broadleaved trees, evergreen	1034.2
Cultivated and managed areas	824.1
Broadleaved trees, deciduous	718.1
Needleleaved trees, deciduous	707.3
Needleleaved trees, evergreen	703.5
Shrub cover, evergreen	685.8
Tree cover/natural vegetation	651.3
Cropland/natural vegetation	606.8
Mixed leaf trees	577.3
Regularly flooded area	482.3
Shrub cover, deciduous	429.2
Herbaceous cover	171.3
Sparse vegetation	56.9
Bare areas	17.5

productivities between 124 and 231 g C m⁻² per year were presented by Lu et al. (2004). In the same study, rice was found to have annual productivity of 632 g C m⁻² and other agricultural areas 492 g C m⁻².

Wang et al. (2008) analysed NPP of Chinese forest areas for the late 1990s and found NPP of $1,372 \text{ g C m}^{-2}$ for evergreen broadleaved forest, $1,240 \text{ g C m}^{-2}$ for evergreen needleleaved forest, 994 g C m^{-2} for deciduous broadleaved forest, and 852 g C m^{-2} for deciduous needleleaved forest. The available NPP data for similar vegetation types are in general consistent with the results obtained in our study (Table 13.2).

13.3.2 *Monthly NPP Patterns*

Figure 13.6 shows mean monthly NPP for China for the period 1999–2012. The monthly NPP values clearly identify variances in productivity for different parts of the country throughout the year.

The warm temperate climate in the southeast of China allows for vegetation productivity throughout the year. In the north and west pronounced winter dormancy can be observed, which lasts from November through March.

In April and May, high productivities of up to 330 g C m^{-2} are reached in the agricultural areas in the central eastern part of the country ($32\text{--}36^\circ\text{N}$ and $113\text{--}121^\circ\text{E}$). Forest areas, which have highest annual NPP in general (Table 13.2), reach maximum productivities a bit later, with about 210 g C m^{-2} per month in June/July/August. Vegetation growth starts later in the northeast of China. In this area, productivity can be observed from May on. The maximum NPP is reached in July and August in the northeastern part of the country. After the maximum, productivity quickly declines within 1 month. Highest productivity for grasslands and cultivated and managed areas in the very northwest of China can be observed in June and July.

Table 13.3 summarizes mean monthly NPP for vegetated land cover classes within China for the period 1999–2011. The results from BETHY/DLR clearly show the different temporal behaviour of evergreen and deciduous trees and shrubs (Table 13.3). Evergreen trees and shrubs show a longer growth period than deciduous trees/shrubs, but the maximum productivity, reached around July, is higher for deciduous trees/shrubs. Evergreen vegetation tends to show a slightly later maximum. This becomes also obvious in Fig. 13.7, which displays mean monthly NPP for the vegetated land cover classes with largest coverage within China.

Maximum vegetation productivity is reached in July or August for almost all analysed land cover classes. A late productivity peak in August can be observed for cultivated and managed areas (Table 13.3).

13.3.3 *Interannual NPP Variability*

Figure 13.8 shows annual NPP for China for individual years from 1999 to 2012 calculated with BETHY/DLR. Differences in NPP distribution between the years

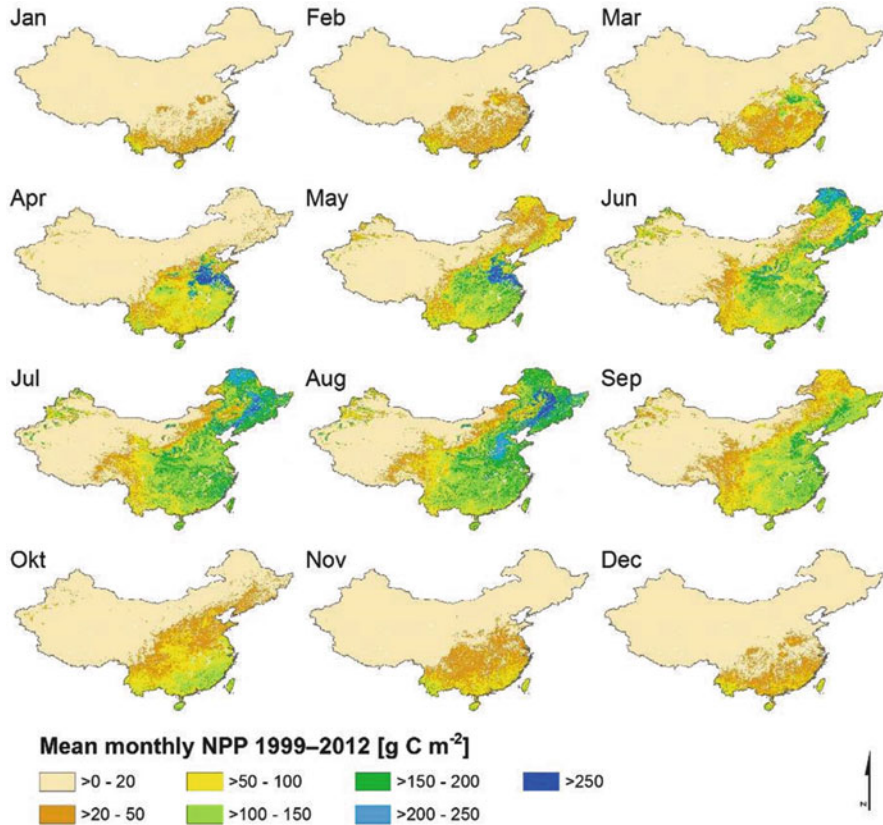


Fig. 13.6 Mean monthly NPP for China for the time period 1999–2012

are clearly visible. The agricultural areas in the central East, for example, show lower productivity in 2000, 2002, and 2003 than in the other years. Boreal forest areas in the northeast have comparatively lower productivities in 2003 and 2011. For the area near the coast in Southeast China higher productivities can be observed in 2003, 2004, 2011 and 2012, compared to the other years.

Interannual NPP variation for individual Chinese provinces is also displayed in Fig. 13.9. The provinces are grouped into regional clusters and mean values for the defined regions are also shown. The graphs allow analysing temporal NPP patterns in more detail. For the dry western part of China, with generally very low NPP, we can observe a slight trend towards higher productivity in the 13-year period analysed in this study (Fig. 13.9). This is not the case for most other regions, where interannual variation is more pronounced. Strong variations can be observed for some districts in the Central North and Southeast. In the northern districts, annual NPP is relatively stable or shows a slight increase. In the Northeast, higher values can be observed for the period 2004–2007. An increase in NPP, followed by a slight downward trend between 2005 and 2011 can be observed for most districts

Table 13.3 Mean monthly NPP for different land cover types in China for 1999–2012

Class name	Mean monthly NPP [g C m^{-2}]											
	Jan	Feb	Mar	Apr	May	Jun	Jul	Aug	Sep	Oct	Nov	Dec
Broadleaved trees, evergreen	29.9	36.4	51.1	87.8	123.1	126.7	140.4	141.7	114.8	90.2	54.3	38.1
Broadleaved trees, deciduous	0.4	1.2	4.5	18.1	79.8	166.4	172.4	156.5	93.3	21.9	3.1	0.6
Needleleaved trees, deciduous	14.3	18.1	28.2	54.5	82.6	93.3	109.8	110.0	83.2	58.0	31.4	20.1
Tree cover, needle-leaved, deciduous	0.0	0.0	1.5	9.5	69.3	195.1	194.8	162.2	67.0	7.6	0.2	0.0
Mixed leaf trees	0.0	0.0	1.9	10.3	60.2	154.4	151.0	127.9	61.4	9.6	0.7	0.0
Tree cover/natural vegetation	36.0	38.2	42.5	60.0	65.5	58.6	63.9	68.2	61.6	63.9	51.2	41.7
Shrub cover, evergreen	14.5	18.2	26.1	53.2	80.5	88.5	102.6	108.7	82.0	58.1	32.7	20.9
Shrub cover, deciduous	1.6	1.6	2.7	11.2	36.6	112.3	120.2	99.1	35.0	4.9	2.1	1.9
Herbaceous cover	0.9	1.2	2.5	6.6	13.8	27.4	42.4	43.2	22.3	7.4	2.5	1.2
Sparse vegetation	0.0	0.0	0.4	2.4	5.1	9.8	14.6	15.1	7.2	1.9	0.2	0.0
Regularly flooded area	8.9	10.5	18.8	34.2	49.2	67.5	90.1	90.4	58.8	28.5	14.9	10.4
Cultivated and managed areas	8.7	13.9	36.0	79.5	100.3	99.0	143.3	161.2	109.9	41.1	19.2	12.0
Cropland/natural vegetation	27.4	27.8	29.6	43.6	55.1	74.0	88.6	89.7	56.1	42.7	40.8	31.4
Bare areas	0.0	0.1	0.4	1.6	2.3	3.1	3.5	3.3	2.1	1.0	0.2	0.0

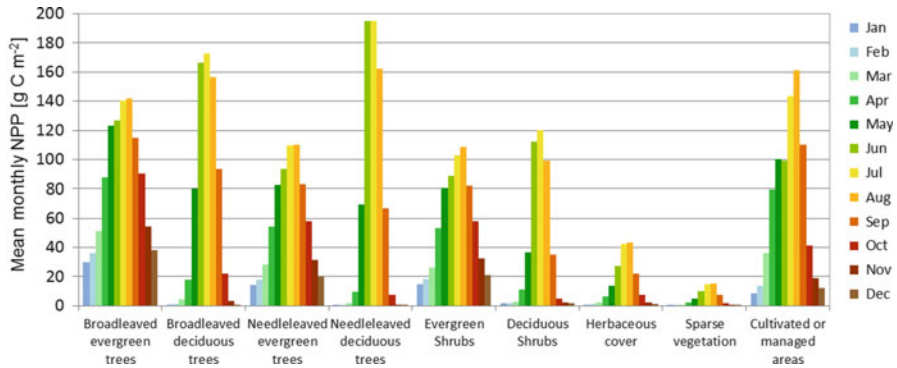


Fig. 13.7 Mean monthly NPP values for 1999–2012 for selected vegetated land cover classes in China calculated with BETHY/DLR

in the Central North and Central South regions. The development of annual NPP in the period 1999–2011 for the district Shanghai differs strongly from the development in the nearby districts. For Shanghai a clear downward trend can be observed in the period of investigation. In the Southwest, NPP values are quite stable, with an increase only for the last year. Annual NPP is more variable in the districts in the Southeast of China.

13.3.4 Impact of Urban Sprawl Around Shanghai

The development of NPP for the province of Shanghai within the observed time-period is remarkable (Fig. 13.9). A linear regression analysis reveals that the downward trend over the course of the observed time span is significant with $p < 0.001$. To quantify the loss of productivity, we calculated mean annual NPP within Shanghai and the two neighbouring prefectural-level cities Suzhou and Jiaxing. The difference between NPP for the years 2000 and 2010 for individual municipalities is displayed in Fig. 13.10. A clear downward trend in NPP can be observed for all municipalities in the area of investigation around Shanghai (Fig. 13.10). Absolute NPP loss is highest in the municipalities Fengxian, Jinshan, and Pinghu at the northern shore of Hangzhou Bay and Jiaxing, with a loss greater than 250 g C m^{-2} in the 10-year period. Relative loss is in general lowest with less than 20 % for the Jiaxing (Southwest), except for the area around the city of Jiaxing. Shanghai (East) and Suzhou (Northwest) have higher percentage NPP reduction. All municipalities except Shazhou in Suzhou have a loss of greater than 20 %. Five out of nine municipalities around Shanghai show a loss of more than 25 % in the period 2000–2010 (Fig. 13.10).

To ensure that years compared are representative and no extraordinary extreme years, we also calculated mean values over the 3-year periods of 1999–2001 and

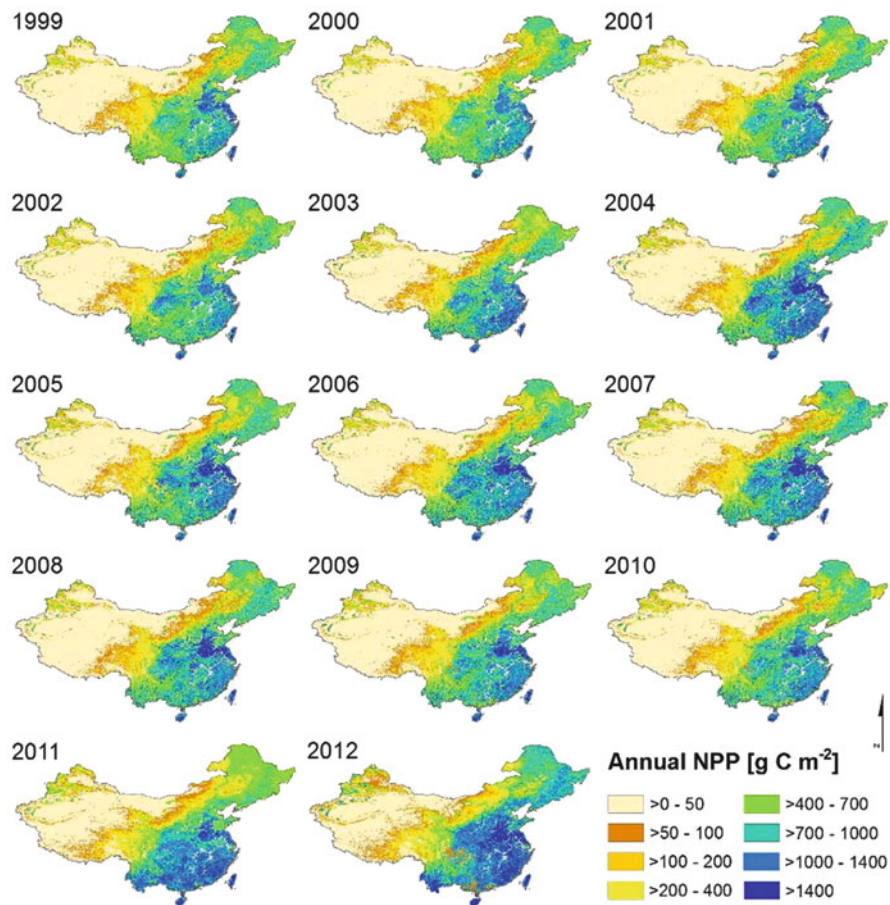


Fig. 13.8 Annual NPP for China for the years 1999–2012 calculated with BETHY/DLR

2010–2012. The results of this periodical comparison and resulting absolute and relative NPP loss values are given in Table 13.4.

The low absolute loss in NPP around the city centre of Shanghai can be explained by the already high urban sprawl in that area. Low absolute loss but high relative loss, such as observed for Baoshan and Minhang (Fig. 13.10), indicate that the area had already been closely built-up in 2000 and that until 2010 large parts of the remaining vegetation areas have been cleared. In general, we assume that a strong decrease in NPP has probably been caused by increasing urban growth. In the case of Wuxian, the high relative loss is due to the large water body of Taihu Lake. Comparatively low absolute NPP loss can be observed within the prefecture-level city of Jiaxing. This region is more rural and large areas are used for agriculture. NPP loss is not as severe as in other parts of the investigated area, but also a reduction of at least 10 % can be observed for the period 2000–2010.

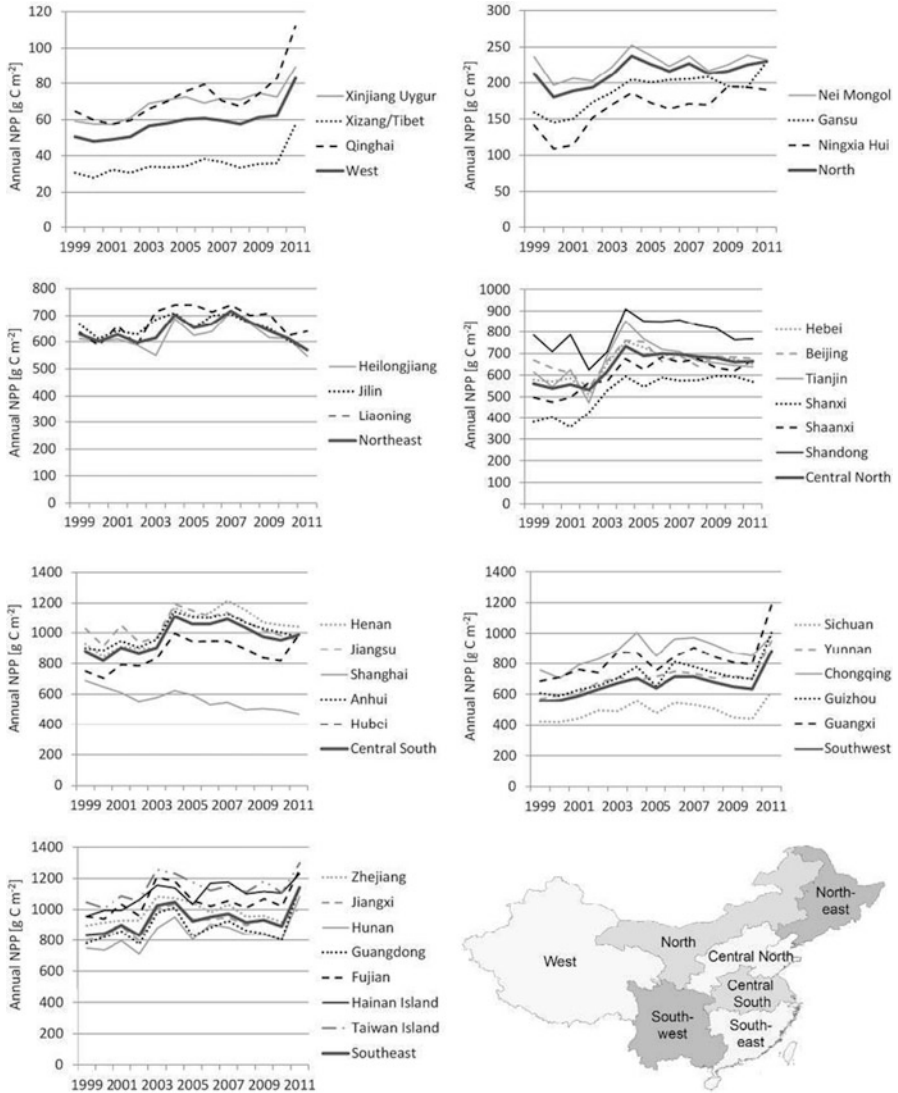


Fig. 13.9 Interannual variation in NPP for various regions in China within the time period 1999–2011. The *thick solid line* in each diagram gives the mean annual NPP variation for each region. The other lines show mean annual NPP for individual provinces. The figure in the lower right shows the location of the regions within China

13.3.5 Monitoring Forest Disturbance in North China

Figure 13.11 depicts a forested region in Northeast China at the border to Russia, which is mainly covered by needle-leaved forest. The area covers the northern part

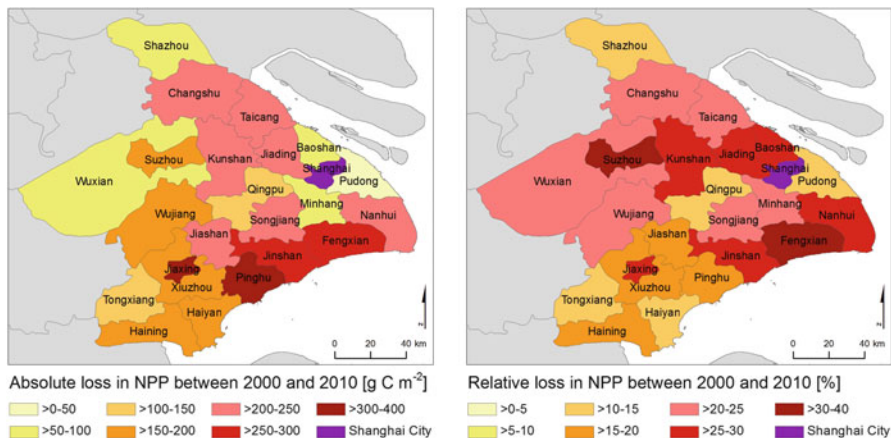


Fig. 13.10 Loss in NPP between 2000 and 2010 for individual municipalities within Suzhou, Jiaxing, and Shanghai. The city centre of Shanghai is shown in violet. *Left:* Absolute loss in annual NPP. *Right:* Relative loss in annual NPP with respect to the annual NPP in 2000

of the Greater Khingan mountains. The area belongs to the provinces Nei Mongol (West) and Heilongjiang (East). The three maps in Fig. 13.11 show annual NPP for the years 2002, 2003, 2006 and 2011. From the NPP data shown in Fig. 13.11, it can be seen that in the year 2003 three forest areas (red polygons) plus some smaller areas have been disturbed. In 2006, an additional area with recent disturbance can be observed (blue polygon in Fig. 13.11).

Figure 13.12 shows average annual NPP for 1999–2011 for the three polygons that were disturbed in 2003. From the annual variation in NPP, the disturbance impacts become also obvious. The vegetation productivity for these areas was high between 1999 and 2002 and suddenly dropped to low values in 2003.

The annual NPP data also clearly show the regrowth of vegetation within the three disturbed areas from 2003. After the rapid decrease in the year of the disturbance event, an increase of annual productivity can be observed. For all three disturbed areas, NPP went up again. The most quickly raise shows largest disturbed area close to the Russian border in the Northeast (forest area no. 1).

The forest disturbances we observe in this study based on the NPP data, have also been reported by Tao et al. 2013, who analysed causes of forest disturbance in Northeast China. The two large disturbance areas in 2003 (no. 1 and 2 from Fig. 13.11) as well as the forest disturbance area in 2006 have been caused by forest fires. The small area in 2003 (no. 3 from Fig. 13.11) can be attributed to deforestation and land-use change (Tao et al. 2013).

Table 13.4 Three-year average mean annual and monthly NPP for individual municipalities within Suzhou, Jiaxing, and Shanghai for the periods 1999–2001 and 2010–2012

	Municipality	3-year mean NPP 1999–2001 [g C m ⁻²]	3-year mean NPP 2010–2012 [g C m ⁻²]	Absolute loss [g C m ⁻²]	Relative loss [%]
Suzhou	Changshu	982.4	804.4	178.0	18.1
	Kunshan	960.6	667.9	292.7	30.5
	Shazhou	720.8	645.4	75.4	10.5
	Suzhou	534.8	375.6	159.2	29.8
	Taicang	1088.0	882.2	205.7	18.9
	Wujiang	745.3	599.3	146.1	19.6
	Wuxian	360.0	284.5	75.5	21.0
Shanghai	Baoshan	187.5	132.7	54.8	29.2
	Fengxian	1048.7	786.3	262.4	25.0
	Jiading	863.6	646.9	216.7	25.1
	Jinshan	1464.7	1123.2	341.5	23.3
	Minhang	279.3	224.2	55.1	19.7
	Nanhui	911.0	694.9	216.1	23.7
	Pudong	267.0	238.0	29.0	10.9
	Qingpu	952.5	797.1	155.4	16.3
	Songjiang	1100.6	879.3	221.3	20.1
Jiaxing	Haining	1181.9	997.2	184.7	15.6
	Haiyan	1388.3	1218.8	169.5	12.2
	Jiashan	1210.3	938.3	272.0	22.5
	Jiaxing	1079.3	842.4	236.9	22.0
	Pinghu	1542.1	1272.8	269.3	17.5
	Tongxiang	1204.3	1080.5	123.8	10.3
	Xiuzhou	1334.4	1149.9	184.5	13.8
Total	ALL	930.8	751.4	165.1	19.8

13.4 Conclusions

We applied the model BETHY/DLR to calculate NPP time-series for China for 14 years from 1999 to 2012. The NPP results were analysed regarding spatial, monthly, and interannual variations. We first presented mean annual NPP distribution for 1999–2012 and derived mean productivities for different land cover classes. The results obtained with BETHY/DLR correspond well to previously published data.

The results of the monthly NPP analyses show, that the data are well suited to analyse differences in temporal patterns of vegetation productivity, both for different regions in China and for different vegetation types. The results are important base information for understanding growth efficiency of different plants in differing climatic regimes.

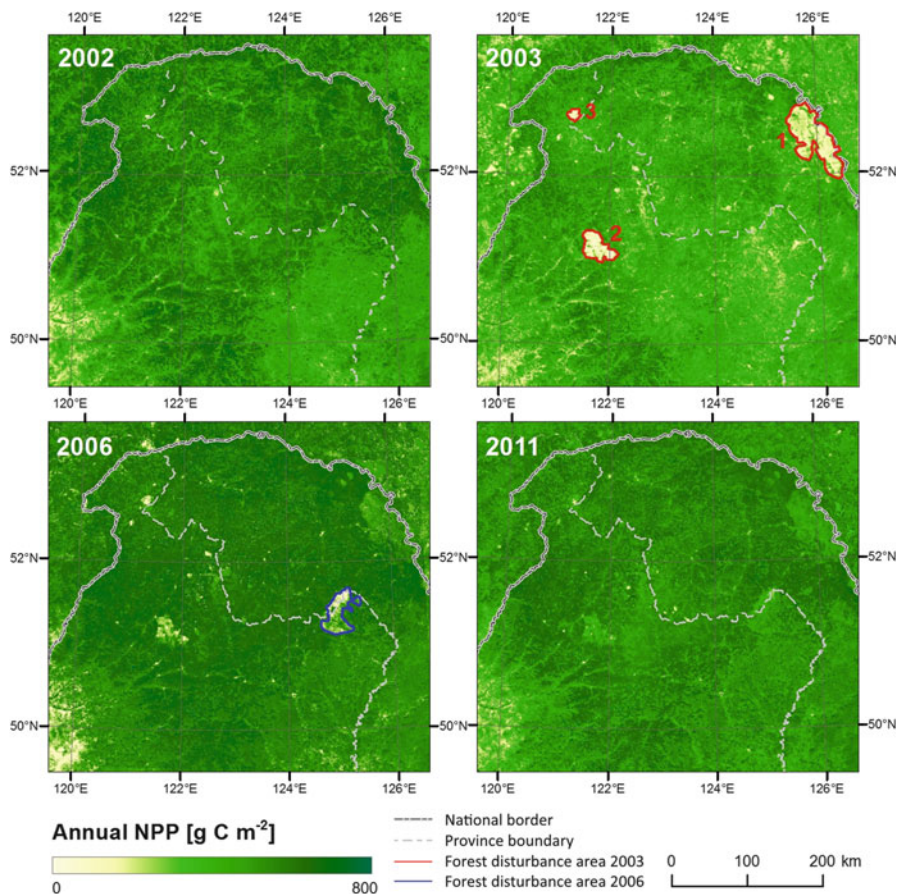


Fig. 13.11 Annual NPP for the years 2002, 2003, 2006, and 2011 for a forest region in North China. The displayed region borders Russia to the North (national border shown as *grey line*). The *red* and *blue* polygons highlight forest disturbance areas in 2003 and 2006 respectively. The numbering of disturbed forest areas in 2003 refers to Fig. 13.12

The analyses of interannual NPP variability provided an interesting insight to the development of annual vegetation productivity within the period under investigation. The annual productivity within different provinces varied considerably. For different regions of China, partly opposite trends could be observed. A decrease in NPP can be observed for the district Shanghai, which differs from the pattern in the surrounding region. This shows the strong influence of urbanization around one of Asia's fastest growing megacities on the environment.

A closer look at the region around Shanghai revealed that a strong impact on the environment can be observed based on the NPP time-series. For Suzhou, Jiaying, and Shanghai, a decrease in vegetation productivity can be observed for the period 2000–2010. All municipalities in the area of investigation around Shanghai showed

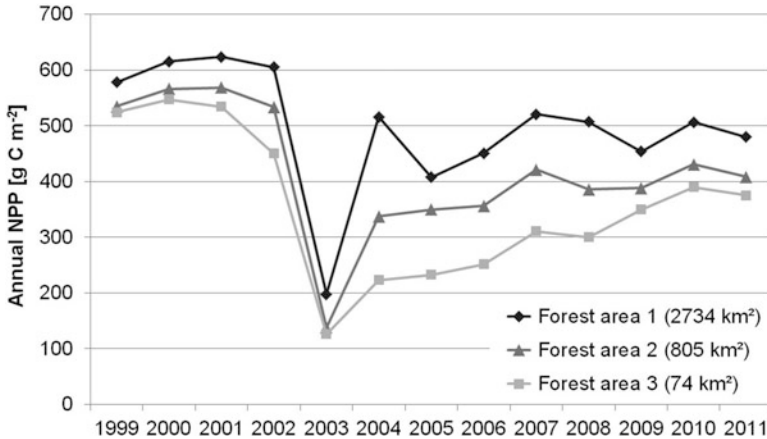


Fig. 13.12 Mean annual NPP for 1999–2011 within the three forest areas from Fig. 13.11 that were disturbed in 2003

a loss in NPP of at least 10 %. In our results, the strong influence of urbanization on the environment around one of Asia’s fastest growing megacities becomes obvious.

The NPP time-series was also analysed for a region in North China. This forest area has been effected by forest fires and logging activity. Our analyses show that the NPP data can be used to identify and monitor areas of forest disturbance. The information derived from NPP time-series can support understanding impacts, speed of regrowth, and status of forests after disturbance events. The derived datasets and presented results of this study provide valuable information about spatial distribution and temporal variation of vegetation productivity in the various regions of China.

Acknowledgements We thank ECMWF, VITO, and IIASA for providing input data for NPP modelling.

References

- Bartholomé E, Belward AS (2005) GLC2000: a new approach to global land cover mapping from Earth observation data. *Int J Remote Sens* 26(9):1959–1977
- Berrisford P, Dee D, Poli P, Brugge R, Fielding K, Fuentes M, Kallberg P, Kobayashi S, Uppala S, Simmons A (2011) The ERA-Interim archive. In: ERA report series, no. 1, version 2.0. ECMWF, Reading
- Cao M, Prince SD, Li K, Tao B, Small J, Shao X (2003) Response of terrestrial carbon uptake to climate interannual variability in China. *Glob Chang Biol* 9:536–546
- Collatz GJ, Ribas-Carbo M, Berry JA (1992) Coupled Photosynthesis–stomatal conductance model for leaves of C₄ plants. *Aust J Plant Physiol* 19(5):519–538
- Dee DP, Uppala SM, Simmons AJ, Berrisford P, Poli P, Kobayashi S, Andrae U, Balmaseda MA, Balsamo G, Bauer P, Bechtold P, Beljaars ACM, van de Berg L, Bidlot J, Bormann N,

- Delsol C, Dragani R, Fuentes M, Geer AJ, Haimberger L, Healy SB, Hersbach H, Hólm EV, Isaksen L, Kållberg P, Köhler M, Matricardi M, McNally AP, Monge-Sanz BM, Morcrette JJ, Park BK, Peubey C, de Rosnay P, Tavolato C, Thépaut JN, Vitart F (2011) The ERA-Interim reanalysis: configuration and performance of the data assimilation system. *Q J R Meteorol Soc* 137(545):553–597
- Eisfelder C, Kuenzer C, Dech S, Buchroithner MF (2013) Comparison of two remote sensing based models for regional net primary productivity estimation – a case study in semi-arid Central Kazakhstan. *IEEE J Select Topics Appl Earth Obs Remote Sens* 6(4):1843–1856
- Eisfelder C, Klein I, Niklaus M, Kuenzer C (2014) Net primary productivity in Kazakhstan, its spatio-temporal patterns and relation to meteorological variables. *J Arid Environ* 103:17–30
- FAO et al (2009) Harmonized world soil database (version 1.1). FAO/IIASA, Rome/Luxemburg
- Farquhar GD, Caemmerer S, Berry JA (1980) A biochemical model of photosynthesis in leaves of C3 species. *Planta* 149(1):78–90
- Feng X, Liu G, Chen JM, Chen M, Liu J, Ju WM, Sun R, Zhou W (2007) Net primary productivity of China's terrestrial ecosystems from a process model driven by remote sensing. *J Environ Manag* 85(3):563–573
- Fu Y, Yu X, Zhao Y, Zeng X, Xia L (2013) Assessment impacts of weather and LandUse/Land Cover (LULC) change on Urban Vegetation Primary Productivity (NPP): a case study in Guangzhou, China. *Remote Sens* 5:4125–4144
- Gao Q, Yu M, Wang J, Jia H, Wang K (2004) Relationship between regional primary production and vegetation patterns. *Ecol Model* 172:1–12
- Gao Y, Zhou X, Wang Y, Wang C, Zhan Z, Chen L, Yan J, Qu R (2013) Vegetation net primary productivity and its response to climate change during 2001–2008 in the Tibetan Plateau. *Sci Total Environ* 444:356–362
- Gio-GL (2013) Gio global land component – Lot 1 “Operation of the global land component”, Product user manual, Leaf Area Index (LAI) – version 1. Issue 11.00. http://land.copernicus.eu/global/sites/default/files/products/GIO-GL1_PUM_LAIV1_11.00.pdf. Accessed 18 Dec 2013
- Hijmans RJ, Cameron SE, Parra JL, Jones PG, Jarvis A (2005) Very high resolution interpolated climate surfaces for global land areas. *Int J Climatol* 25:1965–1978
- Hou Y, Wang S, Zhou Y, Yan F, Zhu J (2013) Analysis of the carbon dioxide concentration in the lowest atmospheric layers and the factors affecting China based on satellite observations. *Int J Remote Sens* 34(6):1981–1994
- Knorr W (1997) Satellite remote sensing and modelling of the global CO₂ exchange of land vegetation: a synthesis study. PhD dissertation. Max-Planck-Institute for Meteorology, Hamburg
- Kottek M, Grieser J, Beck C, Rudolf B, Rubel F (2006) World map of the Köppen-Geiger climate classification updated. *Meteorol Z* 15:259–263
- Lu L, Li X, Veroustraete F, Dong QH (2004) Estimation of NPP in Western China using remote sensing and the C-Fix model. In Proceedings of IEEE international geoscience and remote sensing symposium, IGARSS 2004, 20–24 September, pp 12–15
- Lu L, Li X, Veroustraete F, Kang E, Wang J (2013) Analysing the forcing mechanisms for net primary productivity changes in the Heihe River Basin, north-west China. *Int J Remote Sens* 30(3):793–816
- Matsushita B, Tamura M (2002) Integrating remotely sensed data with an ecosystem model to estimate net primary productivity in East Asia. *Remote Sens Environ* 18(1):58–66
- Niemeijer C (2002) Developing indicators for environmental policy: data-driven and theory-driven approaches examined by example. *Environ Sci Policy* 5(2):91–103
- PRB (2013) 2013 world population data sheet. http://www.prb.org/pdf13/2013-population-data-sheet_eng.pdf. Accessed 29 Jan 2014
- PRC (2012) The People's Republic of China national report on sustainable development, 100 pp. <http://www.china-un.org/eng/zt/sdeng/P020120608816288649663.pdf>. Accessed 27 Nov 2013

- Prentice IC, Farquhar GD, Fasham MJR, Goulden ML, Heimann M, Jaramillo VJ, Khashgi HS, Le Quéré C, Scholes RJ, Wallace DWR (2001) The carbon cycle and atmospheric carbon dioxide. In: Houghton JT, Ding Y, Griggs DJ, Noguer M, van der Linden PJ, Dai X, Maskell K, Johnson CA (eds) *Climate change 2001: the scientific basis. Contribution of working group I to the third assessment report of the Intergovernmental Panel on Climate Change*. Cambridge University Press, Cambridge/New York
- Schimel DS (1995) Terrestrial biogeochemical cycles: global estimates with remote sensing. *Remote Sens Environ* 51(1):49–56
- Tao J, Zhang Y, Yuan X, Wang J, Zhang X (2013) Analysis of forest fires in Northeast China from 2003 to 2011. *Int J Remote Sens* 34(22):8235–8251
- UNDP (2013) *China national human development report 2013. Sustainable and liveable cities: towards ecological civilization*, p 200. http://www.undp.org/content/dam/china/docs/Publications/UNDP-CH-HD-Publication-NHDR_2013_EN_final.pdf. Accessed 26 Nov 2013
- USGS (1996) GTOPO30, Global 30-Arc-Second Elevation Data Set. U.S. Geological Survey, EROS Data Center, Sioux Falls, South Dakota. http://eros.usgs.gov/#/Find_Data/Products_and_Data_Available/GTOPO30. Accessed 9 Dec 2013
- Wang Y, Zhao P, Ren H, Kakubar Y (2008) Spatiotemporal dynamics of forest net primary production in China over the past two decades. *Glob Planet Chang* 61(3–4):267–274
- Wißkirchen K, Tum M, Günther KP, Niklaus M, Eisfelder C, Knorr W (2013) Quantifying the carbon uptake by vegetation for Europe on a 1 km² resolution using a remote sensing driven vegetation model. *Geosci Model Dev Dis* 6:2457–2489
- Yan J, Wang Y, Zhou G, Zhang D (2006) Estimates of soil respiration and net primary production of three forests at different succession stages in South China. *Glob Chang Biol* 12(5):810–821